Comparative Study of the Bonding in the First Series of Transition Metal 1:1 Complexes M−L (M = Sc, ..., Cu; L = CO, N_2, C_2H_2, CN^-, NH_3, H_2O, and F^-)

Julien Pilme and Bernard Silvi*

Laboratoire de Chimie Théorique (UMR-CNRS 7616), Université Pierre et Marie Curie, 4 Place Jussieu 75252-Paris Cédex, France

Mohammad Esmail Alikhani

Laboratoire de Dynamique, Interactions et Réactivité, (UMR-CNRS 7075), Université Pierre et Marie Curie, 4 Place Jussieu 75252-Paris Cédex, France

Received: June 13, 2005; In Final Form: September 7, 2005

The nature of the chemical bonding in the 1:1 complexes formed by the fourth period transition metals (Sc, ..., Cu) with 14 electrons (N_2, CN^-, C_2H_2) and 10 electrons (NH_3, H_2O, F^-) ligands has been investigated at the ROB3LYP/6-311+G(2d) level by the ELF topological approach. The bonding is ruled by the nature of the ligand. The 10 electrons and anionic ligands are very poor electron acceptors and therefore the interaction with the metal is mostly electrostatic and for all metal except Cr the multiplicity is given by the $[Ar]c^n$ configuration of the metallic core ($n = Z - 20$). The electron acceptor ligands which have at least a lone pair form linear or bent complexes involving a dative bond with the metal and the rules proposed previously for monocarbonyls (*J. Phys. Chem. A* **2003**, *107*, 4506) hold. In the case of ethyne, it is not possible to form a linear complex and the cyclic C_{2v} structure imposed by symmetry possesses two covalent M−C bonds, therefore the multiplicity is given by the local core configuration $[Ar]c^n$ for all metals except Mn and Ni.

1. Introduction

In a recent paper we have shown that the description of the chemical bonding in the 1:1 complexes (M−CO) formed by a first series of transition metal atom (M) and a carbonyl (CO) can be rationalized by very simple chemical considerations.[1] In this work, the information provided by the topological analysis of the electron localization function (ELF) is interpreted in terms of the superposition of Lewis-like mesomeric structures. Let us briefly recall the conclusions we were able to draw:

1. The net electronic charge transfer is from metal to carbonyl as expected from electronegativities. It is on the order of 1 electron, except for Cr− and Cu−CO for which it amounts to 0.6 e.

2. Except those of Cr− and Cu−CO, all complexes are linear in order to minimize the interaction between the C−M bond and the remaining nonbonding valence density of the metal in agreement with VSEPR arguments.

3. For Cr− and Cu−CO the stable core configurations $[Ar]c^5$ and $[Ar]c^{10}$ determine the multiplicity of the ground state, i.e., septet and doublet, respectively.

4. The Cr− and Cu−CO complexes have a bent structure in order to maximize the electron transfer from the metal valence density to the carbonyl ligand.

5. Except for Cr−, Mn−, and Cu−CO, the spin multiplicity of the ground state follows Hund's rule for the $[Ar]c^{n+2}$ ($n = Z - 20$) configuration. This configuration also determines the symmetry of the ground state.

6. The electronic configurations accounting for the charge transfer have to be consistent with $[Ar]c^{n+2}$ with respect to both spin multiplicity and symmetry, therefore the electron transfer toward CO involves one unpaired electron in the left part of the periodic table (Sc, Ti, V) and half an electron pair on the right side (Fe, Co, Ni). The remaining valence electron density follows the same behavior.

7. Mn is the pivot element: it transfers half an electron pair like right side elements and has unpaired free valence density like left side ones. The spin multiplicity is that of the free atom in the ground state as a consequence of this compromise.

In the same paper, we proposed a procedure for the evaluation of "σ donation" and "π back-donation" in the topological scheme and concluded that these concepts are not very useful.

The aim of the present paper is to investigate the bonding in 1:1 transition metal complexes for ligands other than CO in the same way in order to discuss how and to what extent the nature of the ligand determines the electronic structure and the geometry. Conventionally the ligands are classified in two groups: on one hand are the σ donors such as NH_3, H_2O, or F^- and on the other hand are the π acceptors like CO, N_2,C_2H_2, or CN^-. Moreover, within each group there are neutral and anionic ligands for which we can expect different behaviors. The paper is organized as follows: first we present the underlying assumptions enabling the validation of simplified bonding representation consistent with the ELF topological analysis, second we report the results of the analysis for each group of ligands and proposes simple electronic pictures which recover the essential features of the analysis.

2. Interpretation of the Bonding from Topological Properties

There are several ways to describe matter at a microscopic level, and a recent debate[2,3] shows that there is no unanimity even within the community of theoretical chemists. In our

* Corresponding author. E-mail: silvi@lct.jussieu.fr.

10.1021/jp053170c CCC: $30.25
Published on Web 10/14/2005

opinion, there are several levels of understanding which do not mutually exclude one another and which can be linked together by different means. The two most widely used descriptions are those provided by quantum mechanics on one hand and by chemistry on the other hand. Quantum mechanics is a paradigm in the sense of T. Kuhn.[4] From its point of view a molecule is a set of interacting particles (nuclei and electrons) ruled by the Schrödinger equation. The accessible properties are either global observable properties (eigenvalues and expectation values of operators) or density of probability distributions which can also be expressed as expectation values of density operators. Quantum mechanics tells nothing about the chemical bond because it is not an observable. In this approach, the quantum system occupies the entire 3-dimensional position space although it is possible to consider subspaces by making use either of translational symmetry in the case of periodic systems or of the prescriptions used by R. Bader to define an atom in a molecule in the context of open quantum subsets.[5,6]

The description provided by chemistry considers a molecule as an assembly of atoms linked by bonds. An atom in a molecule consists of a core (the nucleus and the inner shell electrons) and of valence electrons in the valence shell. The structure of the core and the possible numbers of electrons belonging to the valence shell are given by the position of the element in the periodic table. In general, a molecule can have fewer electrons than the sum of the populations of the valence shells of its atoms because some of the valence electrons may be shared by two or more valence shells. Such electrons are said to be bonding electrons whereas the remaining valence electrons are nonbonding. The most general arrangement of the electrons among the valence shells constitutes a chemical electronic structure. For a given molecular system, several chemical electronic structures are possible and therefore a weighted sum of these mesomeric structures provides a better description than the unique (expected) dominant structure. In this description, the bonding arises either from shared electrons or from delocalized electrons, i.e., electrons accounting for the difference of the considered valence shells in different chemical structures. One of the aims of Lewis's theory of valence[7,8] is to predict the most probable structures with the help of additional rules such as the octet rule and the rule of two. The Lewis's approach emphasizes the electron pair as a key concept. It is worth noting, that a system containing N electrons has at most $N/2$ pairs in the chemical description and $N(N-1)/2$ in the quantum mechanical one. The chemical approach is not a paradigm, because many concepts lack a clear definition and also because it has no mathematical model behind it.

To establish a bridge between these two descriptions one needs an intermediate representation which is provided either by the quantum chemical approaches (i.e., the MO and VB theories) or by the topological ones. Basically, the quantum chemical approaches which give a chemical meaning to the approximate wave function implicitly violate the postulates of quantum mechanics and suffer additional problems due, for example, to noninvariant quantities, which yield arbitrary choices. As pointed out by Coulson:[9] "This epistemological difficulty is mostly due to the weakness of interpretative methods that give physical significance to quantities, such as molecular orbitals or valence bond structures, appearing as intermediates during the course of approximate procedures of solution of the many-body Schrödinger equation." In the topological approach a partition of the molecular space is achieved by an external mathematical theory, the theory of dynamical systems. This technique builds the basins of the attractors of the gradient vector field of a scalar local function (called potential function by mathematicians) which carries the chemical or physical information. The only decisions to be taken are, on one hand, to accept the dynamical system theory as the partition scheme and, on the other hand, to choose a relevant potential function. In most of the papers published by our group, the electron localization function of Becke and Edgecombe[10] has been used for this purpose. The reasons for this choice are theoretical (ELF is clearly related to the pair functions[10−12] and to the excess kinetic energy due to Pauli repulsion[13,14]) and also pragmatical in nature (ELF is easy to calculate, it is bounded in the $[-1, 1]$ interval, and it yields results which fulfill our expectations). The topology of the ELF gradient field[15,16] evidences two types of basins: the core basins around nuclei with $Z > 2$ and the valence basins in the remaining space. These basins closely match the electronic domains defined by Gillespie in the VSEPR model[17−19] and therefore the ELF gradient field topology provides a reliable mathematical model for Lewis's valence theory as well as for VSEPR. The core basins are denoted by C(A) where A stands for the atomic symbol of the atom to which it belongs whereas V(A, B) denotes a valence basin shared by the A and B atomic centers. This approach has been extensively used for the study of chemical bonding,[20−34] of reactivity,[35−38] and of chemical reactions.[39−45] Moreover, the valence basins are characterized by their synaptic order defined as the number of core basins with which a given valence basin shares boundaries.[20,46] By integrating the one electron density over any of the core or valence basin volumes we calculate their populations $\bar{N}(\Omega_i)$ which can be alternatively defined as the expectation values of the basin population operators. The closure relation of the basin population operators enables statistical analysis of the basins populations to be carried out through the definition of a covariance matrix.[47] In the case of open shell systems, it is also very interesting to localize the unpaired electron by calculating the integrated spin density over localization basins.

Although the topological representation proposes a rather satisfactory interpretation of the bonding, phenomenological descriptions in terms of superposition of mesomeric structures are often very helpful, at least, as explanatory models. As proposed in two previous papers,[47,48] the data provided by the topological analysis can be used to build such models and also to discuss their ability to describe the distribution of the electrons. This implies making the following assessments:

1. Electrons of the valence shell of an atom are distributed among the valence basins of this atom.
2. Nonbonding electrons are assigned to monosynaptic basins.
3. Bonding electrons are assigned to the polysynaptic basin whose label corresponds to the interpenetrating atomic shells.
4. Several electron pairs may be assigned to one basin. To illustrate this procedure we consider the dinitrogen molecule as a pedagogical example. Figure 1 displays the localization domains of this molecule. The population vector and the covariance matrix of the valence basins calculated at the B3LYP/6311+G(2d) level.[49−53]

$$\begin{pmatrix} \bar{N}(\mathrm{V(N,N')}) = 3.44 \\ \bar{N}(\mathrm{V(N)}) = 3.28 \\ \bar{N}(\mathrm{V(N')}) = 3.28 \end{pmatrix} \langle \overline{\mathbf{cov}} \rangle = \begin{pmatrix} 1.22 & -0.61 & -0.61 \\ -0.61 & 0.96 & -0.35 \\ -0.61 & -0.35 & \\ 0.96 & & \end{pmatrix}$$

The four mesomeric structures considered are

$$\underset{\mathbf{1}}{\langle \mathrm{N{=}N|} } \quad \underset{\mathbf{2}}{\mathrm{|N{=}N\rangle}} \quad \underset{\mathbf{3}}{\langle \mathrm{N{-}N\rangle}} \quad \underset{\mathbf{4}}{\mathrm{|N{\equiv}N|}}$$

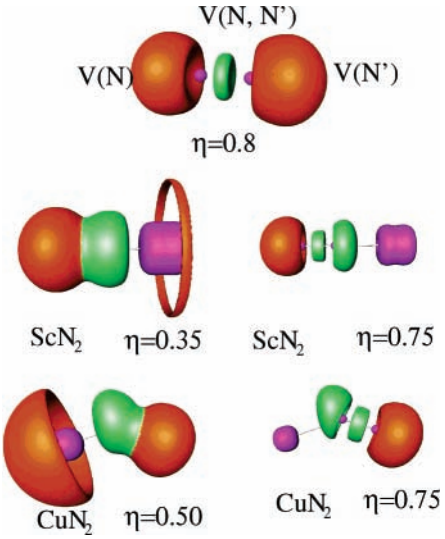

Figure 1. Localization domains of N_2 (top), ScN_2 (middle) and CuN_2 (bottom). Color code: magenta = core, green = valence disynaptic, and red = valence monosynaptic.

Structures **1** and **2** correspond to electron numbers close to the actual basin populations, structure **3** enables the V(N,N′) population to be less than 4, and **4** is the structure which obeys the octet rule. For each of these structures, the number of electrons assigned to the valence basins are

	1	**2**	**3**	**4**
V(N,N′)	4	4	2	6
V(N)	4	2	4	2
V(N′)	2	4	4	2

The respective weights $w_1 = w_2 = 0.31$, $w_3 = 0.33$, and $w_4 = 0.05$ are determined in order to yield populations in good agreement with the reference calculations and reasonable values for the covariance matrix elements. Thus, the population vector and the covariance matrix of this model are

$$\begin{pmatrix} \bar{N}(\mathrm{V(N,N')}) = 3.44 \\ \bar{N}(\mathrm{V(N)}) = 3.28 \\ \bar{N}(\mathrm{V(N')}) = 3.28 \end{pmatrix} \langle \overline{\mathbf{cov}} \rangle = \begin{pmatrix} 1.20 & -0.60 & -0.60 \\ -0.60 & 0.92 & -0.32 \\ -0.60 & -0.32 & \\ 0.92 & & \end{pmatrix}$$

We can be surprised by the weight of the structure **4** in respect to traditional chemical view of the N_2 molecule where the four "π electrons" are mostly attributed to the N−N bond. In the ELF topological framework, the charge contributions of π orbitals to bonding basin V(N,N′) and lone pairs V(N) and V(N′) are fairly equally shared. Moreover, a BOVB calculation carried out by Braïda[54] yields resonance structure coefficients in agreement with this result.

3. Results and Discussion

All the calculations have been performed with the Gaussian 98/DFT quantum chemical package.[55] The DFT calculations have been carried out with Becke's three-parameters hybrid method[49,50] using the Lee−Yang−Parr correlation functional[56] (denoted as B3LYP) within the restricted open shell framework, the molecular orbital being expended for all atoms on the 6-311+G(2d,p) atomic basis sets.[51−53,57,58] According to our previous paper on MCO complexes, the bond dissociation energy (BDE) of each complex has been calculated with respect to the correlated metal state, which is either the ground state ($[Ar]3d^n4s^2$ configuration except Cr and Cu atoms) or the first excited state ($[Ar]3d^{n+1}4s^1$). The topological analysis has been carried out with the TopMod package.[59] In addition to the classical topological population analysis data,[59] namely the basin populations $\bar{N}$, population variances σ^2, and integrated spin densities $\langle S_Z \rangle$ of the high spin component of the multiplet, it is convenient to define the net charge transfer from the metal atom M toward the ligand L as $\delta q = Z(\mathrm{M}) - [\bar{N}(\mathrm{C(M)}) + \bar{N}(\mathrm{V(M)})]$. δq is an useful quantifier of the nature of the bonding since it provides a measurement of the electron density transfer between two molecular fragments.

TABLE 1: Geometrical and Energetic Properties of MN_2 Complexes[a]

M	state	*r*(M−N)	*r*(N−N)	∠MNN	BDE[b]
N_2	$^1\Sigma^+$		109.1		
Sc	$^4\Sigma^-$	209.6	112.3	180.0	146.3
Ti	$^5\Delta$	200.9	112.4	180.0	126.2
V	$^6\Sigma^+$	197.8	111.6	180.0	93.6
Cr	$^7A'$	211.7	111.3	146.1	55.6
Mn	$^6\Pi$	202.2	112.2	180.0	83.6
Fe	$^3\Sigma^-$	184.5	111.0	180.0	127.9
Co	$^2\Delta$	171.8	111.3	180.0	224.9
Ni	$^1\Sigma^+$	170.8	111.2	180.0	81.9
Cu	$^2A'$	186.3	110.6	150.2	100.7

[a] Distances are in nm, angles in deg, and bond dissociation energy (BDE) in kJ·mol^{-1}. [b] BDE (kJ·mol^{-1}) = $[E_{N_2} + E_{M(3d^{n+1}4s^1)} - E_{Complex}]$.

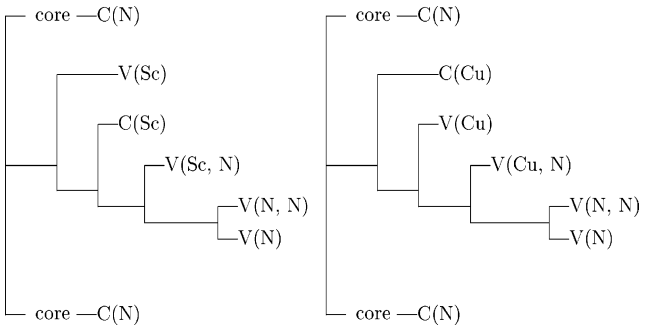

Figure 2. Reduction of localization diagram of ScN_2 (left) and CuN_2 (right).

3.1. MN_2 Complexes. The NiN_2[60−62] and the V−, Cr−, and Mn−N_2[63] complexes have been experimentally studied by infrared spectroscopy in rare gas matrices, and it was concluded that all systems except Cr−N_2 are linear. These results have been supported by DFT calculations[62,63] whereas the iron complex has been studied at both CASSCF[64] and DFT levels.[65,66] For this latter system there is a discrepancy between the results since the ground state is predicted to be $^3\Sigma$ by the CASSCF and BP86 calculations and $^5\Sigma$ by Duarte[66] with another functional (BPW91). Table 1 reports, the B3LYP/6311+G2d optimized geometries and bond dissociation energies (BDE) of the whole series of M−N_2 complexes in their ground state. In the case of Fe−N_2 which is found to have a $^3\Sigma$ ground state, additional B3LYP/6-311+G(3df) and CCSD(T) calculations have been done which confirm that the $^5\Sigma$ state is about 35 kJ·mol^{-1} above the triplet. Except Cr−N_2 and Cu−N_2 which have a bent C_s geometry, all complexes are found to be linear. Moreover, in all cases the spin multiplicity and symmetry of the ground state is the same as in the carbonyl analog.[1]

The localization domains of ScN_2 and CuN_2 are displayed in Figure 1 whereas localization reduction diagrams[20,67] of these complexes (Figure 2 provide patterns similar to those of the MCO series. Table 2 presents the results of the ELF population analysis for the M−N_2 complexes in their ground state, the integrated spin densities correspond to the high spin ($M_S = S$) component of each multiplet. The dinitrogen complexes follow

TABLE 2: Basin Populations $\bar{N}$, Integrated Half-Spin Densities $\langle S_z \rangle$, and Population Differences (Δ) with Respect to Free Dinitrogen N_2 for MN_2 Complexes

		C(M)		V(M)		V(M,N)			V(N,N)		V(N)		
M	state	$\bar{N}$	$\langle S_z \rangle$	$\bar{N}$	$\langle S_z \rangle$	$\bar{N}$	$\langle S_z \rangle$	Δ	$\bar{N}$	Δ	$\bar{N}$	Δ	δq^a
ScN_2	$^4\Sigma^-$	19.19	0.61	0.82	0.41	4.15	0.27	0.93	2.82	−0.54	3.77	0.55	0.99
TiN_2	$^5\Delta$	20.47	1.21	0.78	0.37	3.96	0.22	0.74	2.89	−0.47	3.76	0.54	0.75
VN_2	$^6\Sigma^+$	21.98	1.94	0.40	0.20	3.80	0.19	0.58	3.01	−0.27	3.59	3.57	0.64
CrN_2	$^7A'$	23.23	2.56	0.47	0.21	3.62	0.10	0.40	2.87	−0.49	3.69	0.47	0.30
MnN_2	$^6\Pi$	23.74	2.07	0.61	0.29	3.81	0.10	0.59	3.09	−0.27	3.54	0.32	0.65
FeN_2	$^3\Sigma^-$	24.20	0.91	1.16	0.06	3.66	0.04	0.44	3.22	−0.14	3.52	0.30	0.64
CoN_2	$^2\Delta$	25.69	0.48	0.62	0.00	3.68	0.00	0.46	3.21	−0.15	3.49	0.27	0.69
NiN_2	$^1\Sigma^+$	26.97	-	0.39	-	3.60	-	0.38	3.24	−0.12	3.59	0.37	0.64
CuN_2	$^2A'$	28.06	0.21	0.59	0.19	3.54	0.05	0.32	3.19	−0.17	3.40	0.18	0.35

[a] δq is the net electron density transfer toward the ligand.

TABLE 3: Geometrical and Energetic Properties of MCN^- Complexes[a]

M	state	r(M−C)	r(C−N)	∠MCN	BDE[b]
CN^-	$^1\Sigma^+$		117.2		
Sc	$^2\Delta$	233.6	116.2	180.0	174.9
Ti	$^3\Sigma^-$	221.1	116.4	180.0	178.7
V	$^4\Delta$	211.2	116.4	180.0	200.0
Cr	$^7\Sigma^+$	217.3	116.6	180.0	133.7
Mn	$^6\Sigma^+$	219.1	116.3	180.0	117.3
Fe	$^5\Sigma^-$	209.4	116.2	180.0	162.9
Co	$^4\Sigma^-$	200.0	116.4	180.0	166.1
Ni	$^3\Delta$	193.7	116.4	180.0	172.9[c]
Cu	$^2\Sigma^+$	193.6	116.4	180.0	157.7

[a] Distances are in nm, angles in deg, and bond dissociation energy (BDE) in kJ·mol^{-1}. [b] BDE = $[E_{CN^-} + E_{M(GS)} - E_{Complex}]$. [c] Calculated with respect to the first excited state of metal $^3D(3d^9 4s^1)$.

the rules given in the Introduction for the monocarbonyl series. However, as expected from electronegativities, the net charge transfers toward the N_2 ligand are always smaller than toward CO. This is especially true for the low spin and spin conserved complexes for which the differences usually amount to ca. 0.4 e. As for the monocarbonyl complexes it is possible to interpret the topological population analysis in terms of a superposition of mesomeric structures of the form $[Ar]c^x v^y l^z$ in which c, v, and l stand for the C(M), V(M), and the transferred charge whereas x, y, and z denote the integral occupancies of these basins. The following weights reproduce the calculated values of the populations of the high-spin and low-spin complexes.

ScN_2	$[Ar]c^3$ (18%)	$[Ar]c^2v^1$ (32%)	$[Ar]v^1l^2$ (50%)
TiN_2	$[Ar]c^4$ (22%)	$[Ar]c^3v^1$ (40%)	$[Ar]c^1v^1l^2$ (38%)
VN_2	$[Ar]c^5$ (60%)	$[Ar]c^4v^1$ (02%)	$[Ar]c^2v^1l^2$ (32%)
MnN_2	$[Ar]c^7$ (39%)	$[Ar]c^6v^1$ (28%)	$[Ar]c^2v^1l^2$ (32%)
FeN_2	$[Ar]c^8$ (26%)	$[Ar]c^6v^2$ (58%)	$[Ar]c^4l^4$ (16%)
CoN_2	$[Ar]c^9$ (52%)	$[Ar]c^7v^2$ (31%)	$[Ar]c^5l^4$ (17%)
NiN_2	$[Ar]c^{10}$ (65%)	$[Ar]c^8v^2$ (19%)	$[Ar]c^6l^4$ (16%)

3.2. MCN^- Complexes. There are very few theoretical and experimental studies on M−CN^- complexes. However, in a recent paper Boldyrev has shown[92] the energetic preference of cyanide anion $CuCN^-$ over isocyanide anion $CuNC^-$ by 6.7 kcal/mol at the CCSD(T) level. Although the CN^- ligand is isoelectronic with CO and N_2, the frontier orbitals of CN^- are destabilized in comparison to CO, and consequently, the metal−ligand interaction is weakened. Moreover, Boldyrev concluded that the bonding picture of the $CuCN^-$ complex can be understood as a neutral Cu atom interacting with a closed-shell CN^- ligand, which is experimentally supported by the photoelectron spectroscopy. Table 3 gathers geometrical and energetic results of M-CN^- ground states. All complexes are found to be linear with a $C_{\infty v}$ symmetry. They are in reasonable agreement with the bonding scheme previously proposed. Indeed, the M−C distance is quite larger than in carbonyl and the C−N distance differs only slightly from the C−N distance in the free CN^- moiety. However, the BDE cannot be compared to the MCO systems for which the metal atomic reference is different. Figure 3 shows the formation of $FeCN^-$ system from metal iron ground-state asymptote (^{5}D). Indeed, the complex is generally formed from the metal ground state ($3d^n4s^2$ configuration except Cr and Cu) and consequently, the spin multiplicities of MCN^- systems are different from the MCO systems, which are generally formed from the first excited state $3d^{n+1}4s^1$.

Figure 4 displays the localization domains of the $ScCN^-$ complex which is representative of the whole series. The picture clearly shows the presence of a V(M,C) disynaptic basin which can be interpreted in terms of the formation of a dative bond between the metal atom and the ligand. However, the reduction of localization diagram in Figure 5 significantly differs from that of the MN_2 complexes. In MCN^-, the reducible domain encompassing the core of the metal and the valence attractors first splits into a metal reducible domain (i.e., C(M) and V(M)) and the ligand reducible valence domain whereas in MN_2, the separation of V(M,C) from C(M) occurs once V(M) has been separated. The sequence observed for MCN^- is not consistent with the formation of a dative bond but rather with a strong electrostatic interaction in which the anionic ligand polarizes the metal subunit.

Table 4 presents the population analysis of MCN^- complexes. The net charge transfers δq toward CN^- ligand are always lower than 0.2 e (even negative for Sc−complex). As already mentioned, though the presence of V(M,C) basin should characterize a dative interaction of metal−ligand interaction,

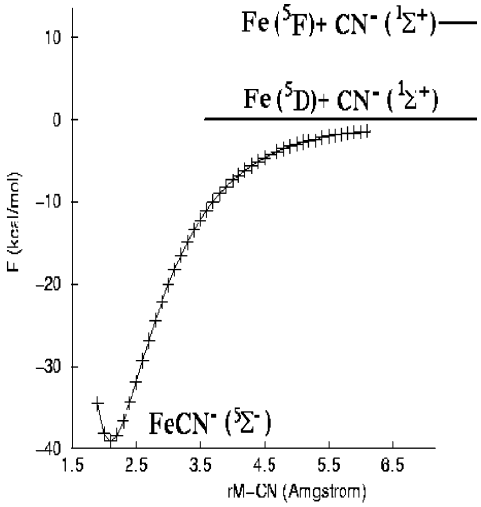

Figure 3. Intermolecular potential energy profile of $FeCN^-$ at B3LYP/6-311+G(2d) level.

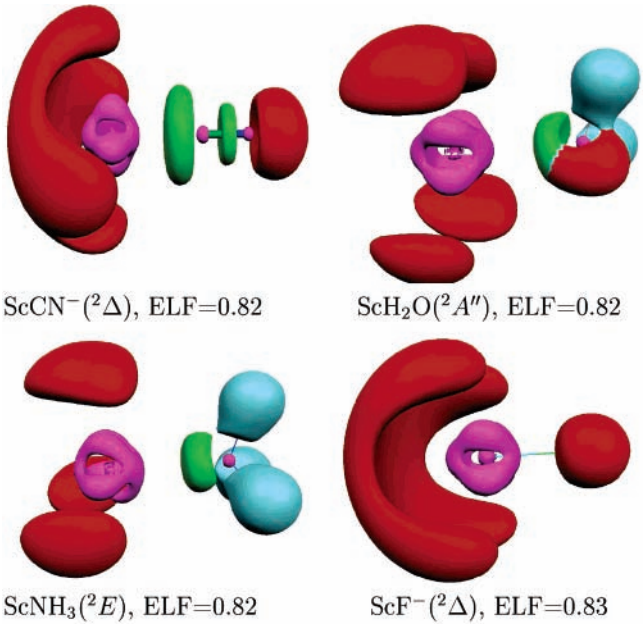

Figure 4. Localization domains of ScL complexes. L = CN^-, H_2O, NH_3. Color code: magenta = core, green = valence disynaptic, red = valence monosynaptic, and light blue = protonated valence disynaptic.

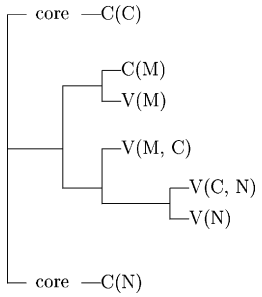

Figure 5. Reduction of localization diagram of MCN^-.

the weak charge transfer (ranging from −0.07 to +0.19 e) contradicts this interpretation and is instead consistent with the "less chemical" bonding scheme M^0-CN^-.

The interpretation of the population analysis data in terms of mesomeric structures yields the following weights:

$ScCN^-$	$[Ar]c^2v^1$ (5%)	$[Ar]c^1v^2$ (72%)	$[Ar]v^3$ (27%)	
$TiCN^-$	$[Ar]c^3v^1$ (4%)	$[Ar]c^2v^2$ (58%)	$[Ar]c^1v^3$ (32%)	$[Ar]c^2v^1l^1$ (6%)
VCN^-	$[Ar]c^3v^2$ (60%)	$[Ar]c^2v^3$ (26%)	$[Ar]c^3v^1l^1$ (14%)	
$CrCN^-$	$[Ar]c^5v^1$ (46%)	$[Ar]c^4v^1l^1$ (52%)	$[Ar]c^4v^2$ (2%)	
$MnCN^-$	$[Ar]c^6v^1$ (25%)	$[Ar]c^6l^1$ (7%)	$[Ar]c^5v^2$ (65%)	$[Ar]c^5v^1l^1$ (2%)
$FeCN^-$	$[Ar]c^7v^1$ (32%)	$[Ar]c^5v^3$ (52%)	$[Ar]c^5v^2l^1$ (16%)	
$CoCN^-$	$[Ar]c^8v^1$ (20%)	$[Ar]c^6v^3$ (66%)	$[Ar]c^6v^2l^1$ (14%)	
$NiCN^-$	$[Ar]c^9v^1$ (31%)	$[Ar]c^8v^2$ (30%)	$[Ar]c^8v^1l^1$ (18%)	$[Ar]c^7v^3$ (21%)
$CuCN^-$	$[Ar]c^{10}v^1$ (64%)	$[Ar]c^{10}l^1$ (11%)	$[Ar]c^9v^2$ (18%)	$[Ar]c^9l^2$ (7%)

Except for Cr, Mn, and Cu, the polarization of the metallic center is achieved by an increase of the V(M) basin at the expense of C(M) thanks to a noticeable contribution of the $[Ar]c^{n-1}v^3$ structure which is the dominant one for Fe and Co. The other important configuration is $[Ar]c^nv^2$ in the Sc, Ti, V,Ni complexes. In the left side of the transition period the multiplicity is driven by the Hund's rule applied to either $[Ar]c^nv^2$ (Sc, Ti, V) or $[Ar]c^nv^1l^1$ in the case of Cr. In the right side it is the $[Ar]c^{n+1}v^1$ configuration which gives the multiplicity. It not possible to derive simple rules giving the symmetry of the total wave function; however, the Δ or Σ symmetries can be understood as minimizing the Pauli repulsion between the ligand and the metallic core.

3.3. $M(C_2H_2)$ Complexes. Though the C_2H_2 ligand is isoelectronic with CO and N_2, the geometry and the electronic structure of its complexes are expected to noticeably differ from those formed by CO and N_2. The topology of ELF in ethyne is characterized by the V(C,C) attractor degenerated on a circle centered at the C−C bond midpoint. The existence of a degenerate (non hyperbolic) critical point implies that the dynamical system is structurally unstable and therefore any appropriate perturbation will remove the degeneracy. Moreover, the V(C,C) basin population is 5.2 e whereas the V(C,H) ones are 2.3 e. In terms of mesomery, this implies a contribution of the $H-C^{\oplus}-C^{\ominus}-H$ and $H-C^{\ominus}-C^{\oplus}-H$ ionic structures on the order of 30%. A C_{2v} structure in which the transition metal forms one bond with each carbon is expected from the ligand properties. To our knowledge, there is no systematic study of the ethyne transition metal complexes. The only structural studies published until now have been carried out experimentally on the copper complex by EPR[68−70] and by infrared spectroscopy in rare gas matrixes.[71] There are also few theoretical studies on the $Ti-C_2H_2$,[72] $Mn-C_2H_2$,[73] $Fe-C_2H_2$,[74] $Ni-C_2H_2$[75−80] and $Cu-C_2H_2$[74,71,81−85] complexes. The geometry of the $M-C_2H_2$ complexes in the C_{2v} geometry is defined by four parameters, namely the metal acetylene distance r(M−C), the C−C bond length r(C−C), the C−H bond length R(C,H), and the ∠CCH angle (see Figure 6). Table 5 reports the electronic structures, the geometrical parameters and the dissociation energies corrected for zero point motion of the $M-C_2H_2$ complexes. Except for Cr, Mn, and Ni, the calculated ground states correspond to the $[Ar]d^ns^2$ configuration of the metal ($n = Z - 20$). The geometries and dissociation energies are in good agreement with the available previous calculations for all metals but copper. For this atom Barone et al.[82,83] reported a weakly bounded C_s complex, the C_{2v} structure corresponding to the transition state of the isomerization reaction belonging to the $^2A_2$ state. Our calculation predicts that the $Cu-C_2H_2$ ground-state belongs to the $^2A_1$ representation; moreover the Cu−C distance for this state, 201 pm, is slightly shorter than that of the $^2A_2$ transition

TABLE 4: Basin Populations $\bar{N}$, Integrated Half-Spin Densities $\langle S_z\rangle$, and Population Differences (Δ) with Respect to Free Cyanide CN^- for MCN^- Complexes

		C(M)		V(M)		V(M,N)			V(N,N)		V(N)		
M	state	$\bar{N}$	$\langle S_z\rangle$	$\bar{N}$	$\langle S_z\rangle$	$\bar{N}$	$\langle S_z\rangle$	Δ	$\bar{N}$	Δ	$\bar{N}$	Δ	δq^a
$ScCN^-$	$^2\Delta$	18.82	0.36	2.25	0.14	2.78	0.00	−0.59	3.62	0.76	3.34	−0.21	−0.07
$TiCN^-$	$^3\Sigma^-$	19.75	0.76	2.24	0.20	2.83	0.04	−0.54	3.65	0.79	3.39	−0.16	0.01
VCN	$^4\Delta$	20.80	1.22	2.14	0.21	2.83	0.07	−0.54	3.65	0.79	3.40	−0.15	0.06
$CrCN^-$	$^7\Sigma^+$	22.46	2.12	1.05	0.51	3.18	0.20	−0.19	3.56	0.71	3.43	−0.12	0.49
$MnCN^-$	$^6\Sigma^+$	23.34	2.30	1.71	0.15	2.75	0.05	−0.62	3.66	0.80	3.38	−0.17	−0.05
$FeCN^-$	$^5\Sigma^-$	23.64	1.49	2.34	0.44	2.81	0.09	−0.58	3.64	0.78	3.39	−0.16	0.02
$CoCN^-$	$^4\Sigma^-$	24.38	0.95	2.49	0.48	2.88	0.06	−0.49	3.63	0.77	3.44	−0.11	0.13
$NiCN^-$	$^3\Delta$	26.02	0.56	1.72	0.35	2.87	0.04	−0.50	3.66	0.80	3.45	−0.10	0.07
$CuCN^-$	$^2\Sigma^+$	27.82	0.13	0.99	0.32	2.93	0.05	−0.44	3.69	0.83	3.43	−0.12	0.19

[a] δq is the net electron density transfer toward the ligand.

TABLE 5: Geometrical and Energetic Properties of $M(C_2H_2)$[a]

M	state	r(M−X)	r(C−C)	r(C−H)	∠HCC	BDE[b]
C_2H_2	$^1\Sigma_g^+$		119.4	106.5		
Sc	$^2A_1$	192.6	133.6	108.9	128.8	171.9
Ti	$^3A_2$	184.5	133.3	108.7	131.8	169.3
V	$^4B_1$	189.0	130.2	108.6	136.4	91.8
Cr	$^5B_2$	182.5	131.6	108.7	134.5	107.6
Mn	$^4A_2$	183.0	129.4	108.3	139.3	−183.8
Fe	$^5B_1$	185.1	125.7	107.4	152.8	−1.2
Co	$^4B_1$	187.1	124.0	107.1	159.2	15.0
Ni	$^1A_1$	170.3	127.6	107.8	148.5	76.1
Cu	$^2A_1$	191.5	122.2	106.7	166.7	110.3

[a] Distances are in nm, angles in deg, and dissociation energy (BDE) in kJ·mol^{-1}. X indicates the midpoint of the C−C segment. [b] BDE is calculated with respect to the ground state of metal.

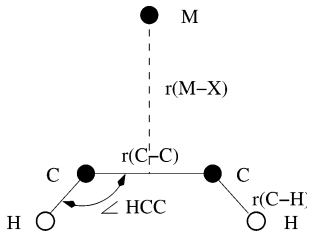

Figure 6. M-C_2H_2. Definition of the structural parameters.

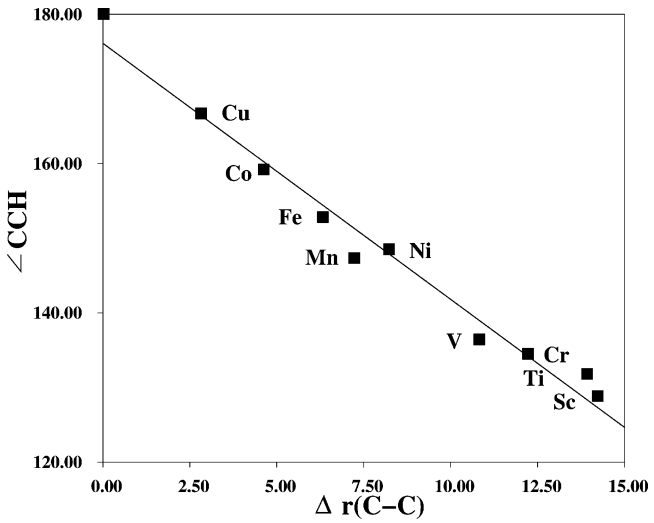

Figure 7. CCH vs Δ r(C−C).

state (248.9 pm). There is a good correlation ($r^2 = 0.98$) between the increase of the C−C bond length and the ∠CCH (Figure 7) which corresponds to the weakening of the C−C bond due to the formation of the M−C bonds.

Figure 8 displays the localization domains of the M−C_2H_2 complexes. In all complexes, the bonding is characterized by the occurrence of two V(M,C) disynaptic basins which correspond to the formation of two covalent bonds and therefore the interaction between the transition metal atom and ethyne cannot be described to a weak π interaction. The basin populations reported in Table 6 clearly indicate the covalent character of the M−C bonds: on one hand, except for Co and Cu, the V(M,C) populations are close to 2, and on the other hand, the integrated spin density is always very small. The monosynaptic V(M) basins have low populations and also contain unpaired density. Schematically the formation of the two M−C bonds is achieved by the donation of an electron pair from the metal atom and of another from the C−C triple bond. The nature of the transferred density implies that either the $[Ar]c^n l^2$ or $[Ar]c^{n-1}l^2v^1$ configuration is involved in the mesomery, therefore, except for Ni, the spin multiplicity of the ground state is given by applying Hund's rule to the $[Ar]c^n l^2$ configuration. For Ni and Cu, it is possible to have the $[Ar]c^{10}$ core configurations, which implies a singlet and doublet ground state for Ni−C_2H_2 and Cu−C_2H_2, respectively.

As shown in Figure 9, the ground state of Sc−C_2H_2 ($^2A_1$) dissociates into an excited doublet state of Sc and ground state of C_2H_2. The most stable structure ($^2A_1$) is indeed stabilized due to its inter-system crossing with the $^2B_2$ state which correlates with the ground states of the fragments. The crossing occurs near to the minimum of $^2B_2$. It is worth noting that the topology of the ELF gradient field near the crossing point is the same for the two states.

3.4. $M(H_2O)$ and $M(NH_3)$ Complexes. The $M(H_2O)$ and $M(NH_3)$ complexes have been observed in the gas phase or at low temperature in matrixes.[93−111] On the other hand, there is an important quantum chemical literature on these systems.[112−121] As the electronic structure of these ligand forbids any π back-donation, the interaction with the metal atom is expected to be weak and dominated by the multipole-induced multipole induction forces. Therefore, one can expect, on one hand, ground-state spin multiplicities identical for complexes and free metal atoms and, on the other hand, geometries similar to those of the hydrogen-bonded complexes of water and ammonia with the metal ligand bond pointing in the direction of a lone pair. The first expectation is verified for all complexes except those of Cr which have a quintet ground-state instead of a septet. The second expectation is confirmed by the values of the optimized geometrical parameters reported in Tables 7 and 8 together with the calculated energetic data of $M(H_2O)$ and $M(NH_3)$ systems in their ground state and which are in reasonable agreement with the previous theoretical studies. The $M(NH_3)$ complexes have a C_{3v} symmetry, while the $M(H_2O)$ ones belong to the C_s point group.

The stability of the $M(H_2O)$ complexes is usually explained by performing the partition of the interaction energy[102] in terms

TABLE 6: Basin Populations $\bar{N}$ and Integrated Half-Spin Densities $\langle S_z \rangle$ with Respect to Free C_2H_2 Molecule for MC_2H_2 Complexes

M	state	C(M)	$S_z(C(M))$	V(M)	$S_z(V(M))$	V(M,C)	$S_z(V(M,C))$	V(C,C)	q(M)
C_2H_2								5.19	
Sc	$^2A_1$	18.78	0.13	0.80	0.30	2.09	0.02	2.93	1.42
Ti	$^3A_2$	19.84	0.58	0.72	0.28	2.10	0.05	2.91	1.44
V	$^4B_1$	21.25	1.19	0.34	0.13	1.89	0.06	3.29	1.41
Cr	$^5B_2$	22.47	1.78			1.97	0.08	3.26	1.53
Mn	$^4B_2$	23.32	1.25	0.22	0.08	1.77	0.06	3.86	1.46
Fe	$^5B_1$	24.02	1.43	0.93	0.39	1.35	0.05	3.75	1.05
Co	$^4A_1$	25.33	1.07	0.89	0.31	0.95	0.02	4.21	0.78
Ni	$^1A_1$	26.57	0.00	0.20	0.00	1.45	0.00	3.74	1.43
Cu	$^2A_1$	27.79	0.18	0.64	0.24	0.49	0.00	4.68	0.57

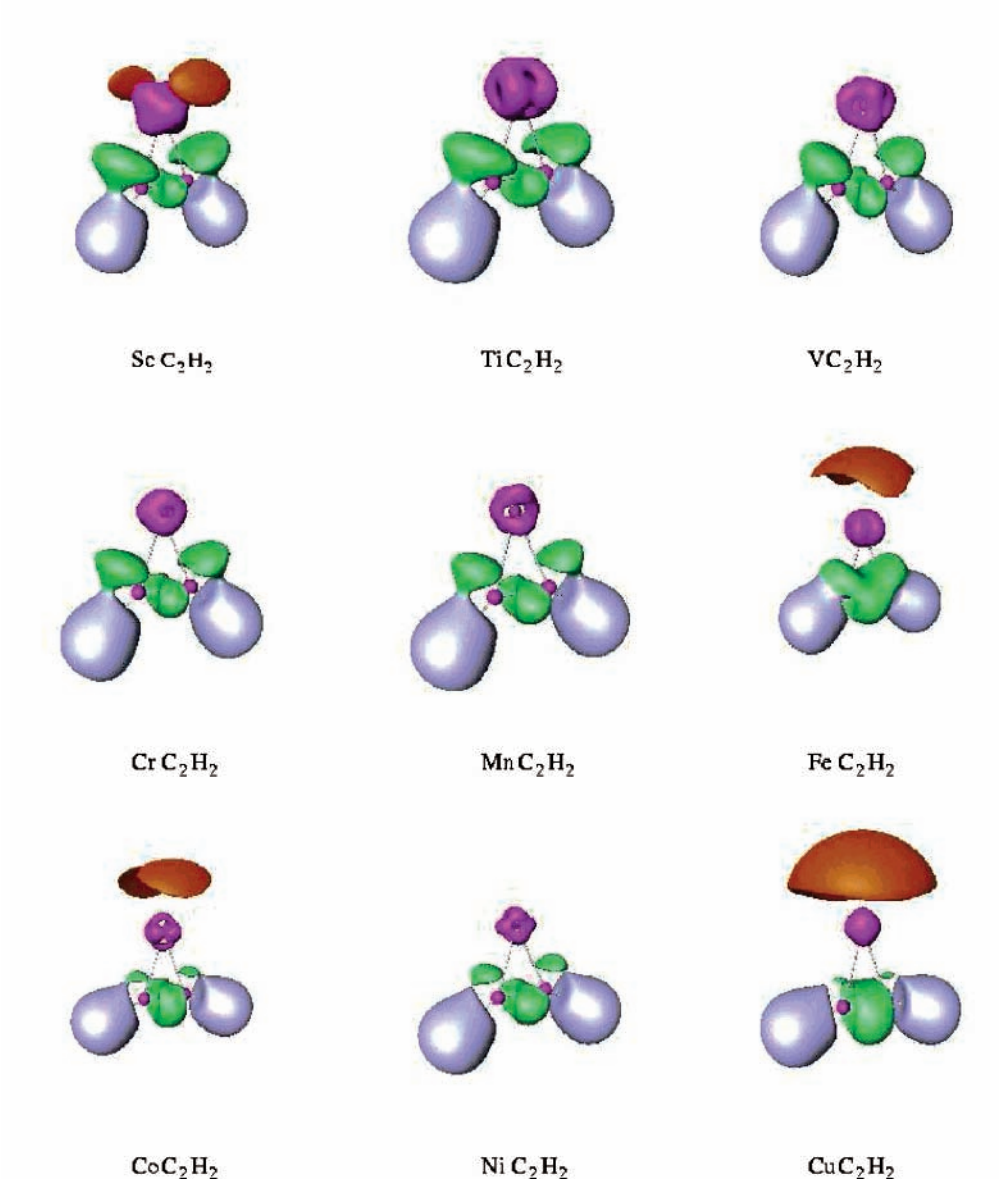

Figure 8. Localization domains of the $M(C_2H_2)$ complexes. Color code: magenta = core, green = valence disynaptic, red = valence monosynaptic, and light blue = protonated valence disynaptic.

TABLE 7: Geometrical and Energetic Properties of $M(OH_2)$[a]

M	state	r(M−O)	∠H−O−H	BDE[b]
H_2O	$^1A'$		105.0	
Sc	$^2A''$	220.4	106.3	60.4
Ti	$^3A''$	214.5	106.6	64.0
V	$^4A'$	210.6	106.1	59.5
Cr	$^5A'$	209.7	105.9	66.8[c]
Mn	$^6A'$	236.2	105.9	12.7
Fe	$^5A''$	225.1	105.7	26.3
Co	$^4A'$	215.0	105.9	34.2
Ni	$^3A'$	213.8	106.1	28.7[d]
Cu	$^2A'$	220.4	105.5	19.6

[a] Distance is in nm, angles in deg, and bond dissociation energy (BDE) in kJ·mol^{-1}. [b] BDE = $[E_{H_2O} + E_{M(GS)} - E_{Complex}]$. [c] Calculated with respect to ^5S state of metal. [d] Calculated with respect to the first excited state of metal (^3D).

TABLE 8: Geometrical and Energetic Properties of $M(NH_3)$[a]

M	state	r(M−N)	BDE[b]
Sc	^2E	230.2	67.0
Ti	$^3A_1$	220.8	77.3
V	^4E	215.7	86.5
Cr	$^5A_1$	212.3	90.4[c]
Mn	$^6A_1$	237.5	28.8[d]
Fe	^5E	223.5	39.5
Co	$^4A_1$	213.9	54.4
Ni	^3E	209.1	52.6[e]
Cu	$^2A_1$	209.2	43.2

[a] Distance is in nm and bond dissociation energy (BDE) in kJ·mol^{-1}. [b] BDE = $[E_{NH_3} + E_{M(GS)} - E_{Complex}]$. [c] Calculated with respect to the ^5S state of metal. [d] Calculated with respect to the ^6D state of metal. [e] Calculated with respect to the first excited state of metal (^3D).

of electrostatic, induction and charge transfer contributions. The stability of ammonia complexes (BDE restricted from 28.8 to 90.4 kcal/mol) is generally greater than that of water complexes (BDE restricted from 12.7 to 66.8 kcal/mol). Siegbahn and Blomberg[122] explain this difference by the diffuse character of the NH_3 lone pair which enhance the dispersion and σ donation contributions.

Figure 4 displays the localization domains of $Sc(H_2O)$ and $Sc(NH_3)$. The two complexes have a disynaptic basin involving the metal, namely V(M,O) and V(M,H). The ELF population

TABLE 9: Basin Populations $\bar{N}$, Integrated Half-Spin Densities $\langle S_z \rangle$, and Population Differences (Δ) with Respect to Free H_2O for MH_2O Complexes

		C(M)		V(M)		V(M, O)			V(O)		
M	state	$\bar{N}$	$\langle S_z \rangle$	$\bar{N}$	$\langle S_z \rangle$	$\bar{N}$	$\langle S_z \rangle$	Δ	$\bar{N}$	Δ	δq^a
Sc	$^2A''$	18.74	0.34	2.15	0.14	2.31	0.00	−0.05	2.41	0.05	0.11
Ti	$^3A''$	19.77	0.78	2.14	0.19	2.22	0.01	−0.14.01	2.46	0.10	0.09
V	$^4A'$	20.80	1.23	2.11	0.23	2.16	0.02	−0.20	2.49	0.13	0.09
Cr	$^5A'$	21.81	1.67	2.08	0.29	2.10	0.02	−0.26	2.55	0.19	0.11
Mn	$^6A'$	22.63	2.18	2.28	0.28	2.24	0.02	−0.12	2.50	0.14	0.17
Fe	$^5A''$	23.84	1.62	2.10	0.34	2.17	0.02	−0.19	2.51	0.15	0.06
Co	$^4A'$	25.01	1.03	1.94	0.42	2.11	0.03	−0.25	2.55	0.19	0.05
Ni	$^3A'$	25.96	0.59	1.99	0.37	2.05	0.02	−0.31	2.58	0.22	0.05
Cu	$^2A'$	27.76	0.16	1.19	0.31	2.19	0.03	−0.17	2.59	0.23	0.05

[a] δq is the net electron density transfer toward the ligand.

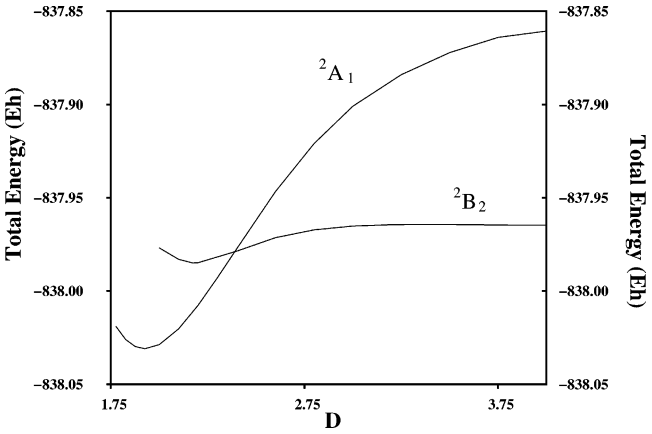

Figure 9. Potential energy curves of the $^2A_1$ and $^2B_2$ states of ScC_2H_2 as a function of the distance between the Sc nucleus and the midpoint of the CC bond (Å).

TABLE 10: Basin Populations $\bar{N}$, Integrated Half-Spin Densities $\langle S_z \rangle$, and Population Differences (Δ) with Respect to Free Ammonia Molecule NH_3 for MNH_3 Complexes

		C(M)		V(M)		V(M,N)			
M	state	$\bar{N}$	$\langle S_z \rangle$	$\bar{N}$	$\langle S_z \rangle$	$\bar{N}$	$\langle S_z \rangle$	Δ	δq^a
Sc	^2E	18.79	0.35	2.11	0.15	2.26	0.00	−0.02	0.10
Ti	$^3A_1$	19.79	0.79	2.15	0.19	2.20	0.02	−0.08	0.06
V	^4E	20.74	1.23	2.12	0.24	2.17	0.03	−0.11	0.14
Cr	$^5A_1$	21.91	1.70	2.11	0.28	2.27	0.02	−0.01	−0.02
Mn	$^6A_1$	23.26	1.98	1.72	0.47	2.13	0.05	−0.15	0.02
Fe	^5E	23.90	1.58	2.04	0.39	2.19	0.03	−0.09	0.06
Co	$^4A_1$	24.76	1.05	2.20	0.41	2.10	0.04	−0.18	0.04
Ni	^3E	25.82	0.60	2.15	0.38	2.08	0.02	−0.20	0.02
Cu	$^2A_1$	27.81	0.13	1.13	0.35	2.16	0.02	−0.12	0.06

[a] δq is the net electron density transfer toward the ligand.

analyses of the water and ammonia complexes reported in Tables 9 and 10 shows the following trends:

1. Except for $CrNH_3$ there is a weak electron density transfer toward the ligand which ranges in 0.02−0.17 e interval. This charge transfer increases the population of the ligand lone pairs with respect to the uncomplexed value. In the case of the water complexes, an additional transfer occurs among the V(M,O) and V(O) basins which enhance the population of the latter at the expense of the former.

2. The population of V(M) basin is greater than or close to 2e (except Cu for which it is 1.19 and 1.13 for H_2O and NH_3, respectively) which implies that the phenomenological mesomeric pictures contains the $[Ar]c^nv^2$ and $[Ar]c^{n-1}v^3$ configurations which determine the spin multiplicity. In the case of the copper complexes, the dominant configuration is $[Ar]c^{n+1}v^1$ which explains why the V(M) basin populations are close to 1.

TABLE 11: Geometrical and Energetic Properties of MF^- [a]

M	state	r(M−F)	BDE[b]
Sc	$^2\Delta$	190.5	359.2
Ti	$^3\Sigma^-$	188.1	327.0
V	$^4\Delta$	184.3	322.1
Cr	$^5\Sigma^+$	183.0	308.6[c]
Mn	$^6\Sigma^+$	190.6	241.7
Fe	$^5\Delta$	184.9	276.8
Co	$^4\Sigma^-$	182.6	208.1
Ni	$^3\Delta$	186.2	217.3[d]
Cu	$^2\Sigma^+$	186.7	187.3

[a] Distance is in nm and bond dissociation energy (BDE) in kJ·mol^{-1}. [b] BDE = $[E_{F^-} + E_{M(GS)} - E_{Complex}]$. [c] Calculated with respect to the ^5S state of metal. [d] Calculated with respect to the first excited state of metal (^3D).

TABLE 12: Basin Populations, $\bar{N}$, and Integrated Half-Spin Densities, $\langle S_z \rangle$, for MF^- Complexes

		C(M)		V(M)		V(F)			
M	state	$\bar{N}$	$\langle S_z \rangle$	$\bar{N}$	$\langle S_z \rangle$	$\bar{N}$	$\langle S_z \rangle$	q(M)[a]	q(F)[b]
Sc	$^2\Delta$	18.90	0.36	2.22	0.13	7.76	0.01	−0.12	−0.88
Ti	$^3\Sigma^-$	19.70	0.76	2.37	0.22	7.77	0.02	−0.07	−0.93
V	$^4\Delta$	20.78	1.22	2.32	0.25	7.76	0.03	−0.10	−0.90
Cr	$^5\Sigma^+$	21.80	1.70	2.26	0.24	7.82	0.06	−0.06	−0.94
Mn	$^6\Sigma^+$	22.95	2.24	2.05	0.17	7.87	0.09	0.00	−1.00
Fe	$^5\Delta$	23.51	1.64	2.58	0.27	7.79	0.09	−0.09	−0.91
Co	$^4\Sigma^-$	24.77	1.03	2.33	0.40	7.79	0.07	−0.10	−0.90
Ni	$^3\Delta$	25.75	0.68	2.37	0.28	7.83	0.04	−0.12	−0.88
Cu	$^2\Sigma^+$	27.57	0.10	1.53	0.37	7.82	0.03	−0.10	−0.90

[a] Net metal charge q(M) = Z(M) − $\bar{N}$(C(M)) − $\bar{N}$(V(M)). [b] q(F) = -1-q(M).

3. The integrated spin density is almost fully localized in the C(M) and V(M) basins.

The nature of metal−ligand interaction can be essentially described as an inductive electrostatic interaction between the permanent moment of the ligand and the induced moment of the metal. The polarization of this latter is testified by the $[Ar]c^{n-1}v^3$ contributions. However, our analysis reveals a small charge transfer toward the ligand which contribute to the stabilization energy.

3.5. MF^- Complexes. To our knowledge there is only one paper[123] discussing a transition metal−F^- complex. However, the calculations carried out at the B3LYP/6-311+G(2d) level indicate that all complexes have found an energetic minimum. The optimized geometrical parameters and the calculated energetic data are presented in Table 11. When the AIM criteria are applied,[5] the M−F^- interaction should be considered as belonging to the closed shell one since the value at the bond critical point of the electron density Laplacian is large and positive whereas that of the density is small.

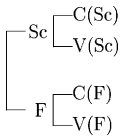

Figure 10. Reduction of localization diagram of ScF^-.

The MF^- complexes have no V(M,F) disynaptic basins. Moreover, the reduction of localization diagram of ScF^- displayed Figure 10 and representative of the whole series clearly indicates that the two moieties are independent chemical systems as the first bifurcation splits the parent reducible domain into two children corresponding respectively to M and F^-. The basin populations and integrated spin densities are reported in Table 11. As a general rule, there is a small electron density transfer toward the metal which amounts at most to 0.12 e. The spin density is almost totally distributed among the metal basins C(M) and basin V(M).

The polarization of the metal atom is achieved by the transfer of electron density from the core basin C(M) toward the metal valence basin V(M) which magnitude reaches 0.58 e in FeF^-. In the mesomeric picture, the $[Ar]c^{n-1}v^3$ configuration accounts for this effect. The spin multiplicity is given by the $[Ar]c^n$ configuration. The total symmetry of the wave function can be modeled by an orbital scheme in which the d_σ orbital has the higher energy, the orbital lower in energy are either the d_δ or the d_π. The order of the d_δ and d_π depends of the occupancy of these latter which must be even. The reverse orbital order (with respect to the usual picture) is a consequence of the electrostatic and Pauli repulsion of the F^- center which stabilizes the orbitals located in a plane perpandicular to the M−F direction.

3.6. Conclusions. The results presented in this paper enable us to propose a classification of the ligands based on their net charges and on their Lewis structures. First, consider the saturated ligands, i.e., those in which there are no multiple bonds. The geometry and the electronic structure of the complexes formed with saturated ligand (F^-, H_2O, and NH_3) is driven by the induction forces. The polarization of the metal is achieved by a transfer of electron density from the core to the valence and, therefore, the $[Ar]c^n$ core configuration determines the spin multiplicity. Though the central atom of these ligands obeys the octet rule, a small electron density transfer toward the ligand lone pair(s) is nevertheless calculated for the two neutral ligands. For F^- the transfer is in the opposite direction.

The unsaturated ligands present multiple bonds in their Lewis structure and therefore are able to accept significant transfer amount of electronic density. The presence of at least a lone pair determines the type of transfer electron density. When the ligand has a lone pair, the density is transferred from the metal to toward the ligand in order to form a dative bond, the number of basins in the ligand part remains constant. It does not matter if it corresponds to the partial transfer of a single electron or an electron pair. The rules derived for the carbonyls recalled in the Introduction hold for the neutral ligands of this family. For CN^-, the charge transfer is almost inhibited and the bonding scheme is close to that already described for saturated ligands. If the ligand has no lone pair (this is the case of ethyne in this paper) the transfer of electron density is achieved by the formation of covalent bonds and therefore an electron pair has to be given by the metal. The electronic structure is determined by $[Ar]c^{n-1}$ core configuration except for Mn and Ni.

These findings provide guidelines to extend this kind of study to other ligands and to the other transition periods in order to validate or invalidate the trends reported here.

Acknowledgment. The authors gratefully acknowledge Prof. R. J. Gillespie for enlighting discussions and for his comments on the draft manuscript.

References and Notes

(1) Pilmé, J.; Silvi, B.; Alikhani, M. *J. Phys. Chem. A* **2003**, *107*, 4506−4514.
(2) Frenking, G. *Angew. Chem., Int. Ed. Engl.* **2003**, *42*, 143−147.
(3) Gillespie, R. J.; Popelier, P. L. A. *Angew. Chem., Int. Ed. Engl.* **2003**, *42*, 3331−3334.
(4) Kuhn, T. *The Structure of Scientific Revolutions*, 3rd ed.; University of Chicago Press: Chicago, IL, 1996.
(5) Bader, R. F. W. *Atoms in Molecules: A Quantum Theory*. Oxford University Press: Oxford, U.K., 1990.
(6) Bader, R. F. W. *Theor. Chem. Acc.* **2001**, *105*, 276−283.
(7) Lewis, G. N. *J. Am. Chem. Soc.* **1916**, *38*, 762−786.
(8) Lewis, G. N. *Valence and the Structure of Atoms and Molecules.* Dover: New York, 1966.
(9) Coulson, C. A. *Valence*; Clarendon: Oxford, U.K., 1952.
(10) Becke, A. D.; Edgecombe, K. E. *J. Chem. Phys.* **1990**, *92*, 5397−5403.
(11) Dobson, J. F. *J. Chem. Phys.* **1991**, *94*, 4328−4333.
(12) Silvi, B. *J. Phys. Chem. A* **2003**, *107*, 3081−3085.
(13) Savin, A.; Jepsen, O.; Flad, J.; Andersen, O. K.; Preuss, H.; von Schnering, H. G. *Angew. Chem., Int. Ed. Engl.* **1992**, *31*, 187−190.
(14) Savin, A.; Nesper, R.; Wengert, S.; Fässler, T. F. *Angew. Chem., Int. Ed. Engl.* **1997**, *36*, 1809−1832.
(15) Silvi, B.; Savin, A. *Nature (London)* **1994**, *371*, 683−686.
(16) Häussermann, U.; Wengert, S.; Nesper, R. *Angew. Chem., Int. Ed. Engl.* **1994**, *33*, 2073−2076.
(17) Gillespie, R. J.; Nyholm, R. S. *Q. Rev. Chem. Soc.* **1957**, *11*, 339−380.
(18) Gillespie, R. J. *Molecular Geometry*; Van Nostrand Reinhold: London, 1972. Gillespie, R. J.; Popelier, P. L. A. *Chemical Bonding and Molecular Geometry*; Oxford University Press: New York, 2001.
(19) Gillespie, R. J.; Robinson, E. A. *Angew. Chem., Int. Ed. Engl.* **1996**, *35*, 495−514. *Chem. Soc. Rev.* **2005**, *34*, 396−407.
(20) Savin, A.; Silvi, B.; Colonna, F. *Can. J. Chem.* **1996**, *74*, 1088−1096.
(21) Silvi, B.; Savin, A.; Wagner, F. R. In *Modelling of Minerals and Silicated Materials*; Silvi, B., D'Arco, P., Eds.; Topics in Molecular Organization and Engineering 15; Kluwer Academic Publishers: Dordrecht, The Netherlands, 1997; pp 179−199.
(22) Noury, S.; Colonna, F.; Savin, A.; Silvi, B. *J. Mol. Struct.* **1998**, *450*, 59−68.
(23) Llusar, R.; Beltrán, A.; Andrés, J.; Noury, S.; Silvi, B. *J. Comput. Chem.* **1999**, *20*, 1517−1526.
(24) Beltrán, A.; Andrés, J.; Noury, S.; Silvi, B. *J. Phys. Chem. A* **1999**, *103*, 3078−3088.
(25) Fuster, F.; Silvi, B. *Theor. Chem. Acc.* **2000**, *104*, 13-21.
(26) Silvi, B.; Gatti, C. *J. Phys. Chem. A* **2000**, *104*, 947−953.
(27) Choukroun, R.; Donnadieu, B.; Zhao, J.-S.; Cassoux, P.; Lepetit, C.; Silvi, B. *Organometallics* **2000**, *19*, 1901−1911.
(28) Chesnut, D. B.; Bartolotti, L. J. *Chem. Phys.* **2000**, *253*, 1−11.
(29) Chesnut, D. B.; Bartolotti, L. J. *Chem. Phys.* **2000**, *257*, 171−181.
(30) Chesnut, D. B. *J. Phys. Chem. A* **2000**, *104*, 7635−7638.
(31) Fressigné, C.; Maddaluno, J.; Marquez, A.; Giessner-Prettre, C. *J. Org. Chem.* **2001**, *65*, 8899−8907.
(32) Noury, S.; Silvi, B.; Gillespie, R. G. *Inorg. Chem.* **2002**, *41*, 2164−2172.
(33) Fourré, I.; Silvi, B.; Sevin, A.; Chevreau, H. *J. Phys. Chem. A* **2002**, *106*, 2561−2571.
(34) Mori-Sánchez, P.; Recio, J. M.; Silvi, B.; Sousa, C.; Mart×c6n Pendás, A.; Luaña, V.; Illas, F. *Phys. Rev. B* **2002**, *66*, 075103.
(35) Fuster, F.; Sevin, A.; Silvi, B. *J. Phys. Chem. A* **2000**, *104*, 852−858.
(36) Fuster, F.; Silvi, B. *Chem. Phys.* **2000**, *252*, 279−287.
(37) Fuster, F.; Sevin, A.; Silvi, B. *J. Comput. Chem.* **2000**, *21*, 509−514.
(38) Silvi, B.; Fuster, F.; Kryachko, E.; Tishchenko, O.; Nguyen, M. T. *Mol. Phys.* **2002**, *100*, 1659−1675.
(39) Krokidis, X.; Noury, S.; Silvi, B. *J. Phys. Chem. A* **1997**, *101*, 7277−7282.
(40) Krokidis, X.; Goncalves, V.; Savin, A.; Silvi, B. *J. Phys. Chem. A* **1998**, *102*, 5065−5073.
(41) Krokidis, X.; Silvi, B.; Alikhani, M. E. *Chem. Phys. Lett.* **1998**, *292*, 35−45.
(42) Krokidis, X.; Vuilleumier, R.; Borgis, D.; Silvi, B. *Mol. Phys.* **1999**, *96*, 265−273.
(43) Krokidis, X.; Moriarty, N. W.; Lester, Jr., W. A.; Frenklach, M. *Chem. Phys. Lett.* **1999**, *314*, 534−542.

(44) Michelini, M. C.; Sicilia, E.; Russo, N.; Alikhani, M. E.; Silvi, B. *J. Phys. Chem. A* **2003**, *107*, 4862−4868.
(45) Berski, S.; Andrés, J.; Silvi, B.; Domingo, L. *J. Phys. Chem. A* **2003**, *107*, 6014−6024.
(46) Silvi, B. *J. Mol. Struct.* **2002**, 1659−1675.
(47) Silvi, B. *Phys. Chem. Chem. Phys.* **2004**, *6*, 256−260.
(48) Lepetit, C.; Silvi, B.; Chauvin. *J. Phys. Chem. A* **2003**, *107*, 464−473.
(49) Becke, A. D. *J. Chem. Phys.* **1993**, *98*, 5648−5652.
(50) Becke, A. D. *J. Chem. Phys.* **1993**, *98*, 1372−1377.
(51) Krishnan, R.; Binkley, J. S.; Seeger, R.; Pople, J. A. *J. Chem. Phys.* **1980**, *72*, 650−654.
(52) Clark, T.; Chandrasekhar, J.; Spitznagel, G. W.; von Ragué Schleyer, P. *J. Comput. Chem.* **1983**, *4*, 294.
(53) Frisch, M. J.; Pople, J. A.; Binkley, J. S. *J. Chem. Phys.* **1984**, *80*, 3265−3269.
(54) Braïda, B. Private communication.
(55) Frisch, M. J.; Trucks, G. W.; Schlegel, H. B.; Scuseria, G. E.; Robb, M. A.; Cheeseman, J. R.; Zakrzewski, V. G.; A. Montgomery, J., Jr.; Stratmann, R. E.; Burant, J. C.; Dapprich, S.; Millam, J. M.; Daniels, A. D.; Kudin, K. N.; Strain, M. C.; Farkas, O.; Tomasi, J.; Barone, V.; Cossi, M.; Cammi, R.; Mennucci, B.; Pomelli, C.; Adamo, C.; Clifford, S.; Ochterski, J.; Petersson, G. A.; Ayala, P. Y.; Cui, Q.; Morokuma, K.; Malick, D. K.; Rabuck, A. D.; Raghavachari, K.; Foresman, J. B.; Cioslowski, J.; Ortiz, J. V.; Baboul, A. G.; Stefanov, B. B.; Liu, G.; Liashenko, A.; Piskorz, P.; Komaromi, I.; Gomperts, R.; Martin, R. L.; Fox, D. J.; Keith, T.; Al-Laham, M. A.; Peng, C. Y.; Nanayakkara, A.; Challacombe, M.; Gill, P. M. W.; Johnson, B.; Chen, W.; Wong, M. W.; Andres, J. L.; Gonzalez, C.; Head-Gordon, M.; Replogle, E. S.; Pople, J. A. *Gaussian 98, Revision A.9.* Gaussian Inc.: Pittsburgh, PA, 1998.
(56) Lee, C.; Yang, Y.; Parr, R. G. *Phys. Rev.* **1988**, *B37*, 785.
(57) Wachters, A. J. H. *J. Chem. Phys.* **1970**, *52*, 1033.
(58) MacLean, A. D.; Chandler, G. S. *J. Chem. Phys.* **1980**, *72*, 5639−5948.
(59) Noury, S.; Krokidis, X.; Fuster, F.; Silvi, B. *Comput. Chem.* **1999**, *23*, 597−604.
(60) Huber, H.; Kuendig, E. P.; Moskovits, M.; Ozin, G. A. *J. Am. Chem. Soc.* **1973**, *95*, 332−344.
(61) Klotzbuecher, W.; Ozin, G. A. *J. Am. Chem. Soc.* **1975**, *97*, 2672−2675.
(62) Manceron, L.; Alikhani, M. E.; Joly, H. A. *Chem. Phys.* **1998**, *228*, 73−80.
(63) Andrews, L.; Bare, W. D.; Chertihin, G. V. *J. Phys. Chem. A* **1997**, *101*, 8417−8427.
(64) Siegbahn, P. E. M.; Blomberg, M. R. A. *Chem. Phys.* **1984**, *87*, 189−201.
(65) Zacarias, A.; Torrens, H.; Castro, M. *Int. J. Quantum Chem.* **1997**, *61*, 467−473.
(66) Duarte, H. A.; Salahub, D. R.; Haslett, T.; Moskovits, M. *Inorg. Chem.* **1999**, *38*, 3895−3903.
(67) Calatayud, M.; Andrés, J.; Beltrán, A.; Silvi, B. *Theor. Chem. Acc.* **2001**, *105*, 299−308.
(68) Kasai, P. H.; McLeod, D., Jr. *J. Am. Chem. Soc.* **1978**, *100*, 625−627.
(69) Kasai, P. H.; McLeod, D., Jr.; Watanabe, T. *J. Am. Chem. Soc.* **1980**, *102*, 179−190.
(70) Chenier, J. H. B.; Howard, J. A.; Miles, B.; Sutcliffe, R. *J. Am. Chem. Soc.* **1983**, *105*, 788−791.
(71) Ozin, G. A.; McIntosh, D. F.; Powers, W. J.; Messmer, R. P. *Inorg. Chem.* **1981**, *29*, 1782.
(72) Zhang, R. Q.; Lu, W. C.; Cheung, H. F.; Lee, S. T. *J. Phys. Chem. B* **2002**, *106*, 625−631.
(73) Swope, W. C.; Schaefer III, H. F. *Mol. Phys.* **1977**, *34*, 1037.
(74) Geurts, P.; Van Der Avoird, A. *Surf. Sci.* **1981**, *102*, 185.
(75) Upton, T. H.; Goddard, W. A. *J. Am. Chem. Soc.* **1978**, *100*, 321.
(76) Geurts, P.; Van Der Avoird, A. *Surf. Sci.* **1981**, *103*, 416−430.
(77) Widmark, P.-O.; Sexton, G. J.; Roos, B. O. *J. Mol. Struct. (THEOCHEM)* **1986**, *28*, 235.
(78) Bofill, J. M.; Pulay, P. *J. Chem. Phys.* **1989**, *90*, 3637−3646.
(79) Mitchell, S. A.; Blitz, M. A.; Fournier, R. *Can. J. Chem.* **1994**, *72*, 587.
(80) Hyla-Kryspin, I.; Koch, J.; Gleiter, R.; T, K.; D, W. *Organometallics* **1998**, *17*, 4724−4733.
(81) Fournier, R. *Int. J. Quantum Chem.* **1994**, *52*, 973.
(82) Barone, V.; Fournier, R.; Mele, F.; Russo, N.; Adamo, C. *Chem. Phys. Lett.* **1995**, *237*, 189−194.
(83) Barone, V.; Adamo, C. *J. Phys. Chem.* **1996**, *100*, 2094−2099.
(84) Böhme, M.; Wagener, T.; Frenking, G. *J. Organomet. Chem.* **1996**, *520*, 31−43.
(85) Legge, F. S.; Nyberg, G. L.; Peel, J. B. *J. Phys. Chem. A* **2001**, *105*, 7905−7916.
(86) Nicolas, G.; Barthelat, J. C. *J. Phys. Chem.* **1986**, *90*, 2870−2877.
(87) Widmark, P.-O.; Roos, B. O. *J. Phys. Chem.* **1985**, *89*, 2180.
(88) Blomberg, M. R. A.; Schüle, J.; Siegbahn, P. E. M. *J. Am. Chem. Soc.* **1989**, *111*, 6156−6163.
(89) Pápai, I.; Mink, J.; Fournier, R.; Salahub, D. S. *J. Phys. Chem.* **1993**, *97*, 9986.
(90) Pierloot, K.; Persson, B. J.; Roos, B. O. *J. Phys. Chem.* **1995**, *99*, 3465.
(91) Kang, Y.; Manceron, L.; Pápai, I. *J. Phys. Chem.* **1997**, *101*, 9650.
(92) Boldyrev, A. I.; X. L.; Wang, L. S. *J. Chem. Phys.* **2000**, *112*, 3627.
(93) Barrett, P. H.; Pasternak, M. *J. Chem. Phys.* **1979**, 71, 3837.
(94) Baggio-Saitovitch, E.; Litterst, F. J.; Micklitz, H. *Chem. Phys. Lett.* **1981**, *3*, 622.
(95) Kauffman, J. W.; Hauge, R. H.; Margrave, J. L. *J. Phys. Chem.* **1985**, *89*, 3541.
(96) Kauffman, J. W.; Hauge, R. H.; Margrave, J. L. *J. Phys. Chem.* **1985**, *89*, 3547.
(97) Mitchell, S. A.; Hackett, P. A. *J. Chem. Phys.* **1990**, *93*, 7822.
(98) Davy, D. R.; Hall, B. M. *Inorg. Chem.* **1988**, *27*, 1417.
(99) Wu, J.; Wesdemiotis, C. *Chem. Phys. Lett.* **1999**, *303*, 243.
(100) Mitchell, S. A. Blitz, M. A.; Siegbahn, P. E. M.; Svensson, M. *J. Chem. Phys.* **1994**, *100*, 1.
(101) Miyawaki, J.; Sugawara, K. *J. Chem. Phys.* **2003**, *119*, 6539.
(102) Pápai, I. *J. Chem. Phys.* **1995**, *103*, 1860.
(103) Chen, M.; Lu, H.; Dong, J.; Mia, L.; Zhou, M. *J. Phys. Chem. A* **2002**, *47*, 11456.
(104) Bauschlicher, C. W., Jr. *J. Chem. Phys.* **1986**, *84*, 260.
(105) Wu, J.; Wesdemiotis, C. *Chem. Phys. Lett.* **1999**, *303*, 243.
(106) Doan, V.; Kasaï, P. A. *J. Phys. Chem. A* **1997**, *101*, 8115.
(107) Szczepanski, J.; Szczesniak, M.; Vala, M. *Chem. Phys. Lett.* **1989**, *163*, 123.
(108) Zhang, L.; Dong, J.; Zhou, L.; Qin, Q. *J. Am. Chem. Soc.* **2001**, *123*, 135.
(109) Zhou, L.; Zhang, L.; Shao, M.; Wang, W.; Fan, K.; Qin, Q. *J. Phys. Chem. A* **2001**, *105*, 5801.
(110) Zhang, L.; Dong, J.; Zhou, L.; Qin, Q. *J. Am. Chem. Soc.* **2000**, *122*, 10680.
(111) Zhang, L.; Dong, J.; Zhou, L. *J. Phys. Chem. A* **2000**, *104*, 8882.
(112) Taylor, M. S.; Muntean, F.; Lineberg, W. C.; McCoy, A. B. *J. Chem. Phys.* **2004**, *121*, 5688.
(113) Mebel, A. M.; Hwang, D. *J. Phys. Chem. A* **2001**, *105*, 7460.
(114) Adamo, C.; Lelj, J. *J. Mol. Struct.* **1997**, *83*, 389.
(115) Tsipis, A. C. *J. Chem. Soc., Faraday Trans.* **1998**, *13*, 437.
(116) Terra, J.; Guenzburger, P. *J. Phys. Chem.* **1995**, *99*, 4935.
(117) Chan, W.; Fournier, R. *Chem. Phys. Lett.* **1999**, *315*, 257.
(118) Adamo, C.; Lelj, F. *THEOCHEM* **1997**, *389*, 83.
(119) Ball, D. W.; Hauge, R. H.; Murgrave, J. L. *Inorg. Chem.* **1989**, *28*, 1599.
(120) Haberlandt, H.; Sauer, J.; Pacchioni, G. *THEOCHEM* **1987**, *34*, 297.
(121) Pasternak, M.; Barrett, P. H. *J. Phys. (Paris)* **1980**, *C-1*, 79.
(122) Siegbahn, P. E. M.; Blomberg, M. R. A.; Svensson, M. *J. Phys. Chem.* **1993**, *97*, 2564.
(123) Schwerdtfeger, P.; Boyd, P. D. W.; Bowmaker, G. A.; Aldridge, L. P. *Struct. Chem.* **1990**, *5*, 405.